

## EXAMINING CONE-SHAPED AND ELLIPTICAL INTERNAL RIBS TO DETERMINE TEMPERATURE DISTRIBUTION AND NUSSELT NUMBER

Dharam Singh Meena\*<sup>1</sup>, Vijaykant Pandey\*<sup>2</sup>

\*<sup>1</sup>M.Tech Research Scholar, RKDF College Of Technology, Bhopal (M.P.), India.

\*<sup>2</sup>Assistant Professor, RKDF College Of Technology, Bhopal (M.P.), India.

### ABSTRACT

A fin is a tiny appendage or component that is connected to a larger body or structure. Fins are often used as foils to provide lift or push, or to guide or stabilise motion when travelling in water, air, or other fluids. Fins are surfaces that protrude from an item in order to improve the rate of heat transfer to or from the environment through increased convection. The quantity of heat transferred by an item is determined by its conduction, convection, or radiation. Heat transfer is increased by increasing the temperature difference between the item and the environment, the convective heat transfer coefficient, or the surface area of the object. Internal shaped fins of various forms have gotten a lot of attention over the last few decades because of their potential advantages over traditional overhead forced heat transfer systems. The intake air velocity, temperature distribution throughout the system, and mass flow rate all have a significant impact on the extended surface heat exchangers. In this work, we are analysing the temperature distribution, nusselt number, and friction factor of their internal fin configuration, which was used for simulation, and it was discovered that sample - 2 with tapered fin enhances better nusselt no. as well as temperature distribution is maximum compared to other fin configurations in the mass flow rate of 0.0395 kg /s.

**Keywords:** Computational Fluid Dynamics, Mass Flow Rate, Internal Shaped Fins, Temperature Distribution, Nusselt Number, Friction Factor.

### I. INTRODUCTION

Fins typically act as foils, providing lift or thrust as they move through water, air, or other fluids, or providing the ability to control or stabilize movement. Ribs are also used to increase surface area for heat transfer purposes or simply as an ornament. Fins first evolved into fish as a means of locomotion. The fish's fins are used to generate thrust and subsequently control its movement. Other aquatic animals such as fish and whales use their pectoral and caudal fins to actively propel and steer. When swimming, they use other fins, such as the dorsal and anal fins, to ensure stability and refine their maneuvers. A fin is a surface that extends from an object to increase the rate of heat transfer to or from its surroundings by increasing convection.

The amount of conduction, convection, or radiation from an object determines how much heat is transferred. Therefore, adding fins to an object increases its surface area and may be an economical solution to heat transfer problems.

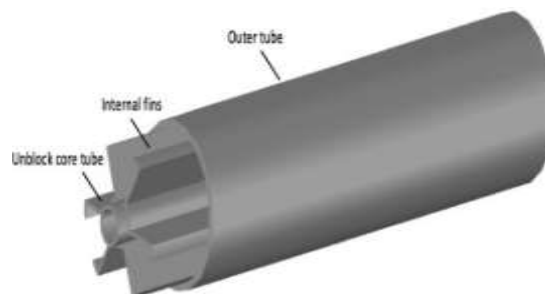


**Figure 1:** Schematic diagram of internal fin tube

### Heat transfer through fins

Fins are extensions on the outer surface of an object that increase the rate of heat transfer to or from the object by increasing convection. This is achieved by increasing the surface area of the body, which increases the heat transfer coefficient significantly. Another possibility is that either the heat transfer coefficient (depending on the type of material used and the conditions of use) or the temperature gradient (depending on the conditions of use) can be increased, so this is an efficient way to increase speed.

Fins are therefore a very popular solution for improving heat transfer from surfaces and are widely used in many objects.

The material of the fins should preferably have a high thermal conductivity. In most applications, the fins are surrounded by a moving liquid that heats or cools rapidly due to their large surface area, and then the high thermal conductivity of the fins allows the heat to rapidly transfer to and from the body. Obtaining optimum heat transfer performance at minimal cost requires calculating the fin dimensions and shape for a specific application, known as fin design. A common way to do this is to create a model of the fin and simulate it under the desired operating conditions.

### **Fin efficiency**

Fin efficiency is one of the critical parameters for materials with high thermal conductivity. A heatsink fin can be thought of as a flat plate through which heat flows from one end and is dissipated into the surrounding liquid on its way to the other end [11]. As heat flows through the fins, the combination of heat sink thermal resistance and convective heat loss impede flow, the temperature of the fins, and thus heat transfer to the fluid from the base to the ends of the fins is reduced. Fin efficiency is defined as the actual heat transferred by the fin divided by the heat transfer if the fin were isothermal (hypothetically, the thermal conductivity of the fin is infinite). Equations 6 and 7 apply to straight ribs.

### **Thermally conductive materials**

Thermal contact resistance is caused by voids caused by surface roughness effects, defects, and interface misalignment. The cavities present at the interface are filled with air. Heat transfer therefore depends on conduction across the actual contact area and conduction (or natural convection) and radiation across the gap. [12] When the contact area is small, such as when the surface is rough, the gap contributes significantly to drag [12]. To lower the contact thermal resistance, the surface roughness can be lowered while increasing the interfacial pressure. However, these improvements are not always practical or possible for electronic devices. Thermal interface materials (TIMs) are a popular way to overcome these limitations. A properly applied thermal interface material replaces the air present in the gap between two objects with a material that has a much higher thermal conductivity. Air has a thermal conductivity of 0.022 W/m K[20], while TIM has a thermal conductivity of 0.3 W/m K[21] or higher. When choosing a TIM, the values provided by the manufacturer should be followed. Most manufacturers give thermal conductivity values for their materials. However, thermal conductivity does not take interfacial resistance into account. Therefore, high thermal conductivity of TIM does not necessarily mean low interfacial resistance. TIM selection is based on three parameters:

The interfacial gap that the TIM must fill, the contact pressure, and the electrical resistance of the TIM. Contact pressure is the pressure exerted at the interface between two materials. Selection does not include material costs. Depending on the details of your electrical design, electrical resistivity can be important.

## **II. LITERATURE REVIEW**

**LufangDuan et al. [1]** investigated the turbulence and heat transfer properties of double-tube structure inner fin tubes and flower-shaped inner fins. A sample containing three flower-shaped lamellae was investigated experimentally and numerically at six different air flow rates and a constant air inlet temperature. The Reynolds number on the air side varied from 3255 to 19580. The simulation results obtained are in good agreement with the experimental data. We subsequently analyzed the effect of geometric finned-tube structures (different number of fins and different core tube diameters) on thermal behavior. As a result, we found that increasing the number of fins resulted in a more uniform distribution of the temperature and velocity fields. The heat transfer performance of the inner finned tube with 3 and 4 petal fins was similar and both were significantly higher than the inner finned tube. With two flower-shaped fins. An optimal ratio of ( $d_o/T_u$  0.28) existed, resulting in better cost-effectiveness. Compared to corrugated fins, petal fins are suitable for operating conditions with tight pressure drop limits, especially in waste heat recovery systems.

**M.J. Lee et al. [2]** In this paper, he experimentally investigated a new type of smooth plate fins with 12 delta winglet vortex generators around each tube of the finned-tube heat exchanger proposed by the authors. To compare the overall properties of the proposed fins with circular corrugated fins, tests are performed on four full-scale heat exchanger surfaces. Two corrugated finned tube heat exchangers (short 10 corrugation and 12 corrugation) with 6 rows of tubes with 2.54 mm or 2.117 mm fin spacing. and two proposed finned-tube heat

exchanger surfaces with five tube rows with equal fin spacing (10-LVG and 12-LVG, respectively). The air-side inlet velocity varies from 1.5 m/s to 7.5 m/s, and the water-side flow velocity is fixed at a constant value at each air inlet velocity. Experimental results show that the heat transfer coefficient and pressure penalty of the heat exchanger surface with the proposed five-row tube fins are almost the same as those of the corrugated heat exchanger surface with six-row tubes. The correlation between the Nusselt number  $Nu$  on the air side and the coefficient of friction  $f$  is obtained. Perform entropy analysis to reveal the thermal amplification mechanism.

**Mohammed. Sikindar Baba et al. [3]** Internal fins in heat exchanger tubes are an excellent way to improve heat transfer. In this article, we report an experimental study of forced convection heat transfer in a double-tube counterflow heat exchanger with multiple internal vertical fins using Fe<sub>3</sub>O<sub>4</sub>-water nanofluids. Enhanced convective heat transfer and pressure drop for nanofluids flowing in horizontal circular tubes with internal vertical fins under turbulent conditions (5300 and volume concentrations of Fe<sub>3</sub>O<sub>4</sub> nanoparticles in the range 0<49200. studied.  $\phi < 0.4\%$ . The results show that the heat transfer coefficient of the finned tube heat exchanger is 80-90% higher than that of the bare tube heat exchanger due to the higher volumetric concentration of nanofluid. The Nusselt number ratio of the Fe<sub>3</sub>O<sub>4</sub>-water nanofluid to the base fluid (water) increases with Reynolds number. The coefficient of friction decreases with increasing Reynolds number and the pressure drop is higher in finned tube heat exchangers than in bare tube heat exchangers due to the effect of the fin geometry resisting flow. The Wilson plot method is used to generate his Nusselt number correlations for his Fe<sub>3</sub>O<sub>4</sub>-water nanofluid flow through a finned tube heat exchanger.

**Swastik Acharya and Sukanta K. [4]**, three-dimensional numerical simulations were performed to predict the flow and temperature fields around a horizontal cylinder with internal fins of natural convection. Varying the fin height, fin spacing or number of fins, and cylinder length at different  $Ra$ , predicting heat loss from a finned cylinder yielded interesting insights. Short Cylinder Heat Loss ( $L/D < 1 > 1$ ) At all fin heights and fin spacings the point of maximum heat loss vanishes. A table was created showing the optimum configuration of fin height and number of fins for maximum heat loss. We found that the mean  $Nu$  of ribbed cylinders decreased with  $H/D$ ,  $L/D$  and increased with  $Ra$ . From the extensive numerical simulations performed in this study, general correlations of  $L/D$ ,  $H/D$ , rib number,  $N$ , and  $Nu$  as a function of  $Ra$  were developed with an accuracy of  $\pm 6\%$ . This is beneficial to the industry. and practical designer.

**Guodong Qiu et al. [5]** Fin-tube evaporators are widely used in air heat pumps. Applying a solar selective absorption coating on the fin surface has been proven to be an effective approach to improve the heat transfer effect of finned tube evaporators using solar energy. However, at present, most attention is paid to improving the performance of heat pump systems using solar energy, and little attention is paid to the heat transfer properties of this type of fins under solar radiation. Therefore, the heat transfer properties of this type of fin under solar radiation were studied using heat transfer theory. Based on the heat transfer model, a theoretical solution for the temperature field was derived and its accuracy was verified by numerical simulations. The effects of various factors on the heat transfer properties of smooth fins have been theoretically analyzed. Results showed that solar radiation reduces convective heat transfer capacity and fin efficiency, and may even account for some of the solar energy dissipated into the environment. The maximum loss of solar energy accounts for about 12.7% of total solar energy, and doubling the fin height only increases the total heat transfer capacity by 60%. Under conditions of high fin height and high insolation, the smaller the convective heat transfer coefficient, the greater the total heat transfer capacity. This study analyzes this kind of heat transfer problem and helps guide the optimized design of finned tube evaporators assisted by solar energy.

**Evangelos Bellows et al.[6]** Parabolic trough collectors are one of the most mature concentrating solar technologies used in many applications. Improving their performance is the key to establishing themselves as viable technologies. The use of internal fins is one of the most interesting techniques for improving flow heat transfer phenomena and improving collector performance. However, using them results in higher pressure losses. The purpose of this work is to investigate the optimal number and placement of lamellae inside the absorber of a parabolic trough collector. The tested lamellae are 10 mm long, 2 mm thick, and rectangular in shape. Different numbers of fins at different positions in the absorber are investigated and the performance of the collector is investigated in each case considering the increase in Nusselt number and coefficient of friction. According to the final result, the inner fin should be placed at the bottom of the absorber where most of the

solar heat flux is concentrated. multi goal This procedure proved that the absorber with three fins at the bottom was the best case with a 0.51% increase in thermal efficiency.

**Mohammad Sepehr et al. [7]** numerically investigated heat transfer, pressure drop and entropy generation in tube bundle and tube coil heat exchangers. The heat transfer coefficient is enhanced by attaching annular fins to the outer surface of the coiled tube. The fluid on the coil side is hot water flowing through the coil at a temperature of 70°C and a flow rate of 1 m/s. On the shell side, on the other hand, dry cooling air flows through the shell side with a temperature of 10 °C and a velocity of 1-4 m/s. The height and number of fins change, as does the velocity of the sheath fluid. The main results of this study are several correlations proposed to estimate the Nusselt number and the shell-side friction coefficient. Additionally, the relationship between NTU, entropy production rate, and thermal efficiency is obtained.

### III. CFD

Computer primarily based simulation is mentioned during this chapter. procedure simulation is technique for examining fluid flow, heat transfer and connected phenomena like chemical reactions. This project uses CFD for analysis of flow and warmth transfer. CFD analysis accepted go in the various industries is employed in R&D and producing of craft, combustion engines and in powerhouse combustion similarly as in several industrial applications.

#### Why computational simulation

Three-dimensional (3D) numerical analysis of whorled coil tubes is dispensed by victimization business CFD tool ANSYS. This can become troublesome and time overwhelming, if this analysis is dispensed by experimentation. Experimental setup is extremely expensive that's why in my work I take facilitate of CFD to create it easier and fewer time overwhelming.

#### Computational fluid dynamics

Computational fluid dynamics, because the name implies, could be a subject that deals with procedure approach to fluid dynamics by means that of a numerical resolution of the equations that cause the fluid flow and though it's known as procedure fluid dynamics; it doesn't simply wear down the equations of the fluid flow, it's conjointly generic enough to be ready to solve at the same time along the equations that direct the energy transfer and similarly the equations that verify the chemical process rates and the way the chemical process takings and mass transfer takes place; of these things may be tackled along in a regular format. So, this define permits America to wear down a really complicated flow circumstances in fairly quick time, specified for a specific set of conditions, associate degree engineer would be ready to simulate and see however the flow is happening and what quite temperature distribution there's and what quite product area unit created and wherever they're fashioned, in order that {we can|we will|we area unit able to} build changes to the parameters that area unit below his management to switch the approach that these items are happening. So, therein sense procedure fluid dynamics or CFD becomes a good tool for a designer for associate degree engineer. it's conjointly a good tool for associate degree associate degree analysis for associate degree examination of a reactor or an instrumentality that isn't functioning well as a result of in typical industrial applications, several things is also happening associate degreeed what a designer has had in mind at the time of fabricating or coming up with the instrumentality won't be really what an operator of the instrumentality introduces into the instrumentality at the time of operation, perhaps once 5 years or 10 years changes might need taken place in between; and in such a case, the presentation of the instrumentality won't be up to the quality and you'd wish to modify it in such some way that you just will restore performance. So, the question is then, what this can managed to the autumn within the performance associate degreeed what quite measures we are able to build while not creating an overall adjustment within the finish of apparatus. Is it potential to urge improved performance from the equipment? Is it potential to extend the productivity? If you wish to appear on of these analysis, then procedure fluid dynamics is employed.

### IV. METHODOLOGY

#### Design procedure of Internal Blossom Shaped Fins

The procedure for solving the problem is

- Modeling of the geometry.
- Meshing of the domain.

- Defining the input parameters.
- Simulation of domain.

Finite volume analysis of Internal Blossom Shaped Fins.

Analysis Type- Fluent.

**Preprocessing**

Preprocessing include CAD model, meshing and defining boundary conditions.

**CAD Model**

**Table 1:** Steel tube dimensions with petal-shaped internal fins

Length of Test section	1000 mm
Outer Diameter	40 mm
Inner Diameter	6 mm
Fin Thickness	2 mm

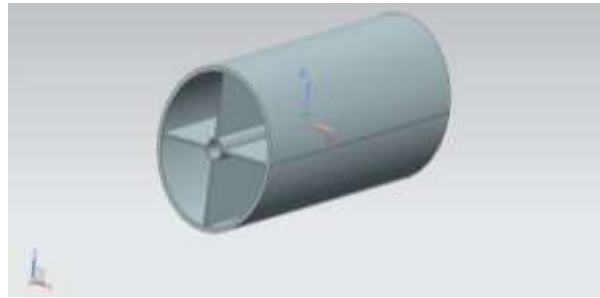


**Figure 2:** CAD Model of petal-shaped internal fins sample 1

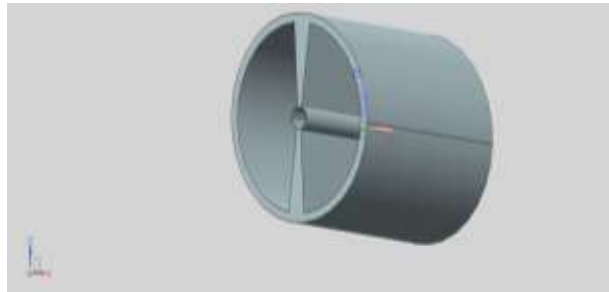


**Figure 3:** CAD Model of petal-shaped internal fins sample 2

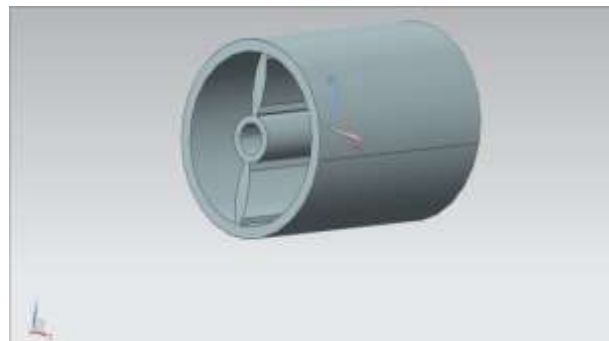


**Figure 4:** CAD Model of petal-shaped internal fins sample 3

**Table 2:** Crosslinking data for organic coatings on steel pipes.

NODES	57625
ELEMENTS	28598

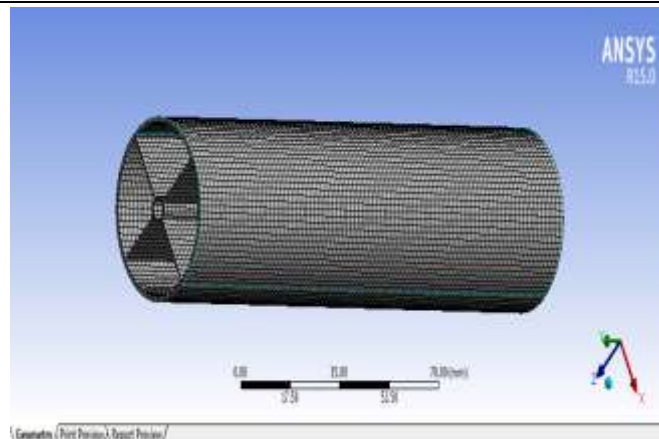


Figure 5: Mesh domain of petal-shaped internal fins sample 1

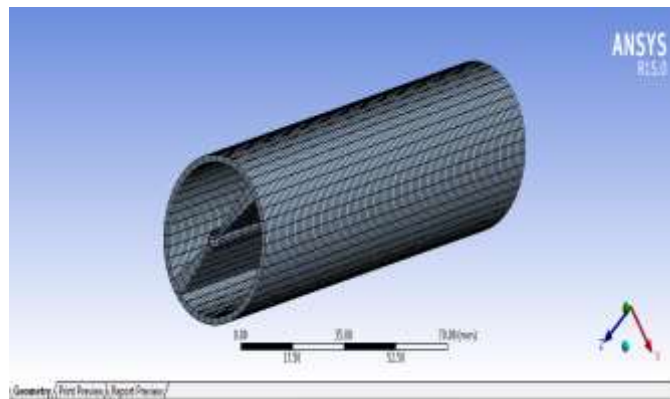


Figure 6: Mesh domain petal-shaped internal fins sample 2

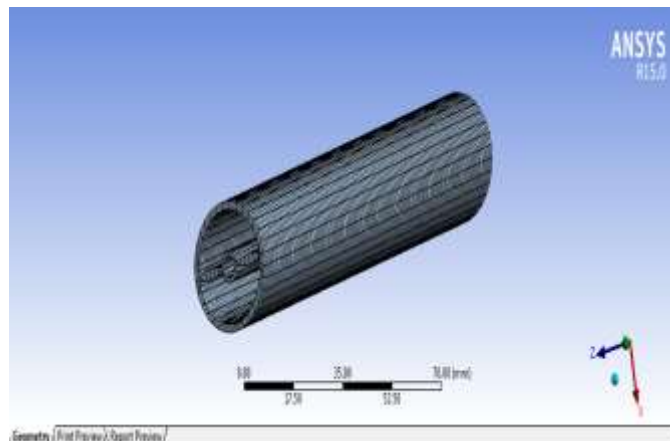
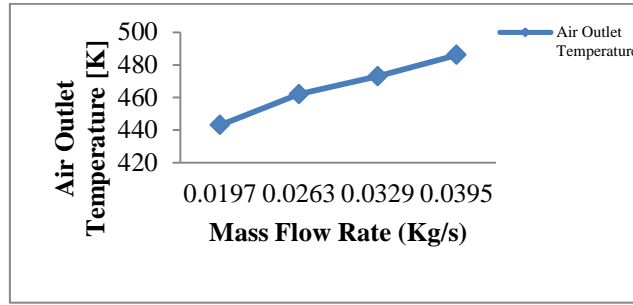


Figure 7: Mesh domain of petal-shaped internal fins sample 3

## V. RESULTS & DISCUSSION

Table 3: Validation result of internal fins for pipe flow by numerical simulation w.r.t mass flow rate.

Air Outlet Temperature	Mass flow rate (Kg/s)
443	0.0197
462	0.0263
473	0.0329
486	0.0395



**Figure 8:** Graph of Air outlet temperature versus mass flow rate

This diagram demonstrates that air outlet temperature number got from CFD Follows the way of air outlet temperature Obtained Experimentally , Average variety of air outlet temperature number in the middle of CFD and Experimentally acquired is 3.76 %.

**Table 4:** Validation result of nusselt number in internal fins for pipe flow by numerical simulation w.r.t mass flow rate.

Nusselt Number	Mass flow rate (Kg/s)
6.35	0.0197
14.87	0.0263
21.52	0.0329
26.65	0.0395

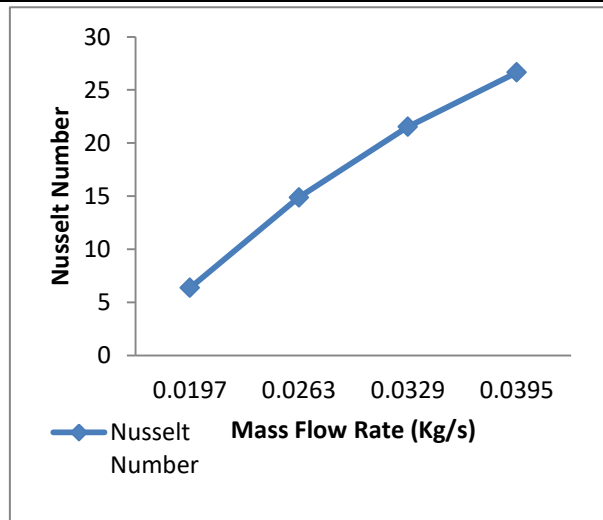


**Figure 9:** Graph of Nusselt number versus mass flow rate

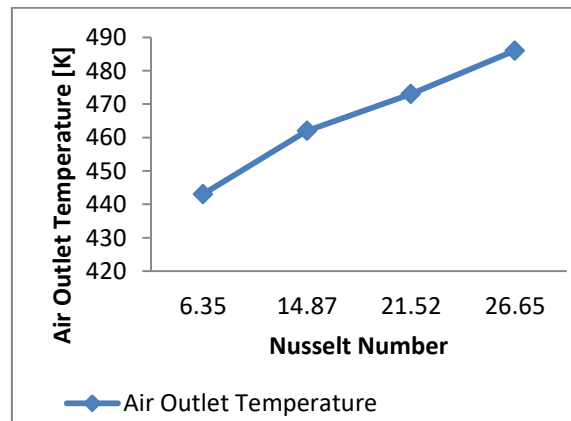


**Figure 10:** Graph of air outlet temperature versus nusselt no.

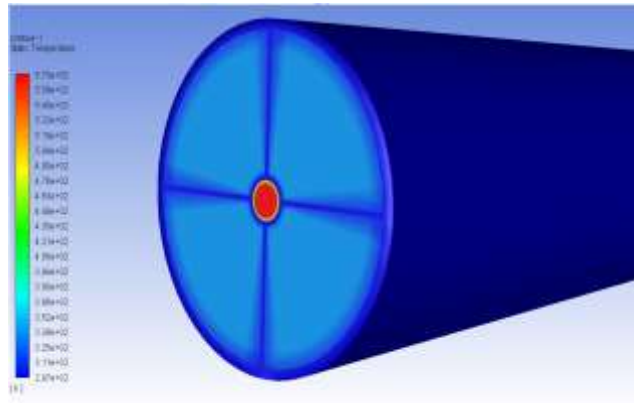


Figure 11: Inlet temperature of internal fins shaped flow

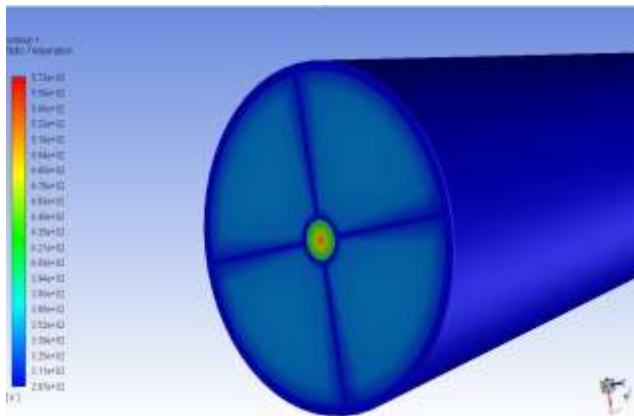


Figure 12: Outlet temperature of internal fins shaped flow

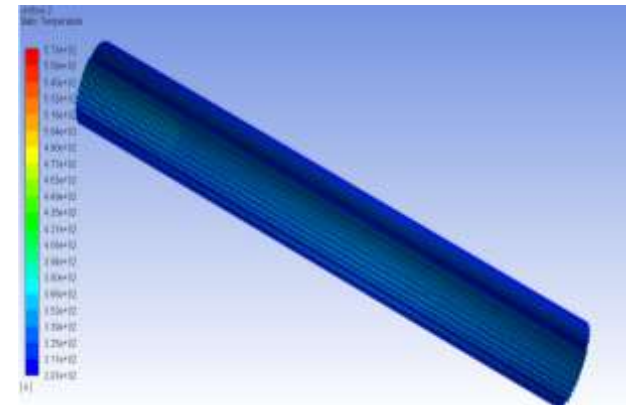


Figure 13: Water temperature distribution domain

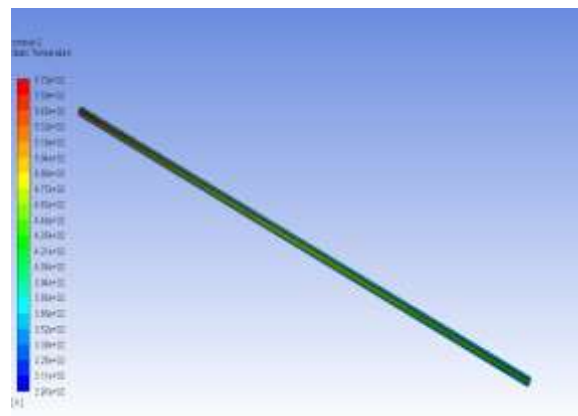
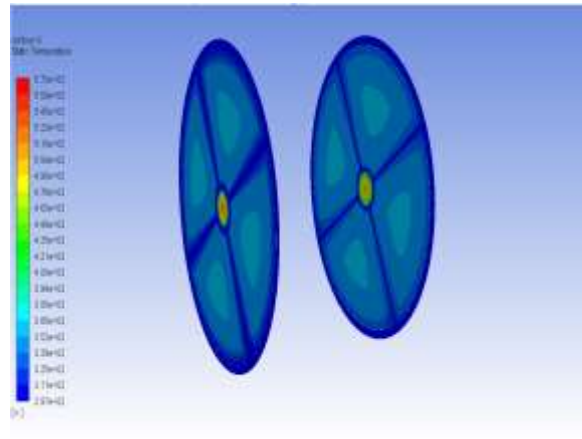


Figure 14: Air temperature distribution domain





**Figure 15:** Temperature distributions on mid-section of pipe flow

Here in this case the temperature at the outlet of the blossom shaped fins is investigated with parallel flow of cold water with hot air, the 4 internal fins temperature distribution is also determined with different mass flow rate and is found that 1.64 kg/s mass flow rate gives optimum solution in the convergence of parallel flow of blossom shaped fins. Different values of temperature of different mass flow rate are shown.

**Table 5:** Showing the different values of Parallel Flow Temperature

Mass flow rate (Kg/s)	Sample 1
0.0197	437
0.0263	455
0.0329	469
0.0395	475

Here in this case the temperature at the outlet of the blossom shaped fins is investigated with sample – 2 parallel flow of cold water with hot air is numerically simulated, the 2 internal tapered fins temperature distribution is also determined with different mass flow rate and is found that sample – 2 is fully converged results compared to other configurations, temperature distribution is shown below.

**Table 6:** Showing the different values of Parallel Flow Temperature

Mass flow rate (Kg/s)	Sample 2
0.0197	423
0.0263	435
0.0329	445
0.0395	458

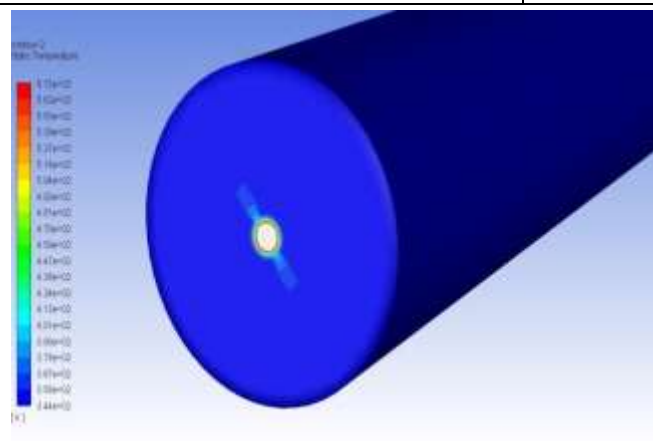


**Figure 16:** Temperature distributions on pipe flow

**Table 7:** Showing the different values of Parallel Flow Temperature

Mass flow rate (Kg/s)	Sample 3
0.0197	429
0.0263	443
0.0329	452
0.0395	467

Here in this case the temperature at the outlet of the blossom shaped fins is investigated with counter flow of cold water with hot air, the 4 internal fins temperature distribution is also determined with different mass flow rate and is found that 1.64 kg/s mass flow rate givs optimum solution in the convergence of counter flow of blossom shaped fins. Different values of temperature of different mass flow rate are shown.

**Table 8:** Showing the different values of Counter Flow Temperature

Mass flow rate (Kg/s)	Sample 1
0.0197	427
0.0263	450
0.0329	463
0.0395	470

Here in this case the temperature at the outlet of the blossom shaped fins is investigated with sample – 2 the counter flow of cold water with hot air is numerically simulated, the 2 internal tapered fins temperature distribution is also determined with different mass flow rate and is found that sample – 2 is fully converged results compared to other configurations, temperature distribution is shown below.

**Table 9:** Showing the different values of Counter Flow Temperature

Mass flow rate (Kg/s)	Sample 2
0.0197	419
0.0263	428
0.0329	437
0.0395	450

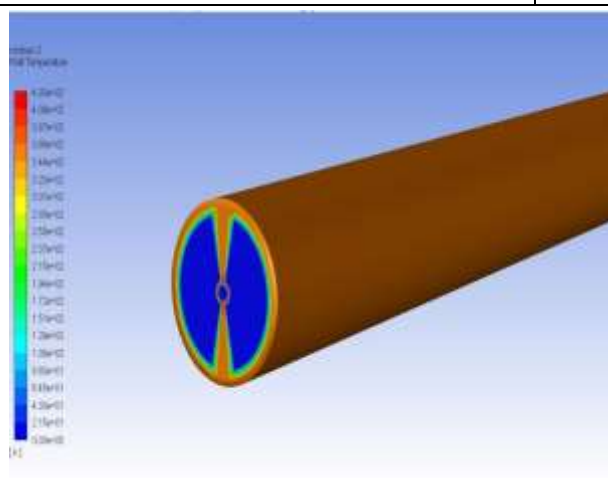


**Figure 17:** Static Temperature distributions on pipe flow

**Table 10:** Showing the different values of Counter Flow Temperature

Mass flow rate (Kg/s)	Sample 3
0.0197	422

0.0263	438
0.0329	446
0.0395	458

**Table 11:** Showing the different values of Parallel Flow Temperature

Parallel Flow Temperature			
Mass flow rate (Kg/s)	Sample 1	Sample 2	Sample 3
0.0197	437	423	429
0.0263	455	435	443
0.0329	469	445	452
0.0395	475	458	467

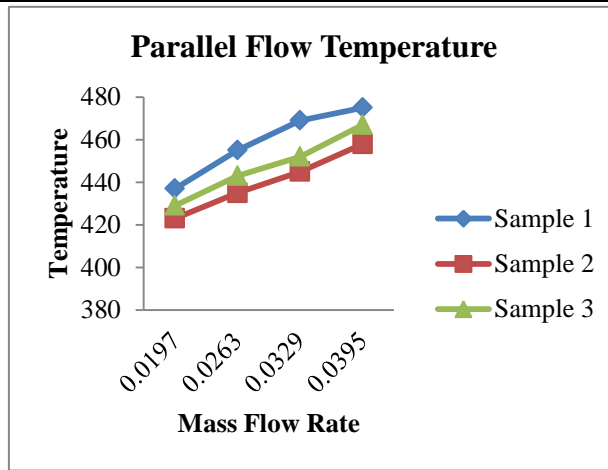


**Figure 18:** Parallel Flow Temperatures

**Table 12:** Showing the different values of Counter Flow Temperature

Counter Flow Temperature			
Mass flow rate (Kg/s)	Sample 1	Sample 2	Sample 3
0.0197	427	419	422
0.0263	450	428	438
0.0329	463	437	446
0.0395	470	450	458

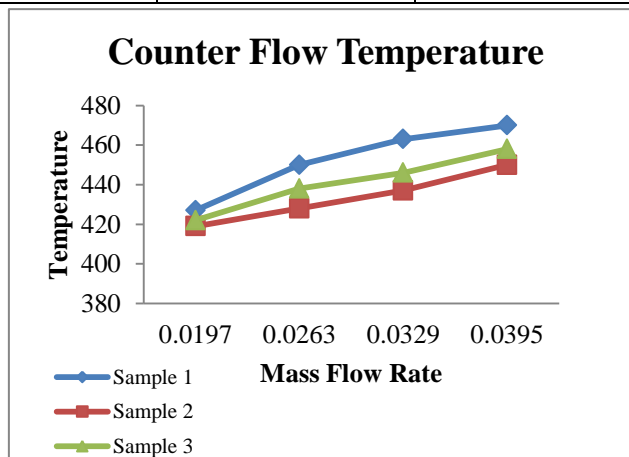


**Figure 19:** Counter Flow Temperature

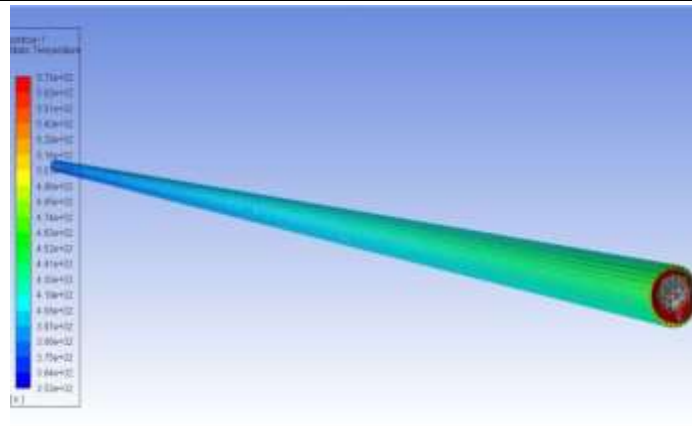


**Figure 20:** Counter Flow Air

Here in this case the nusselt number of the blossom shaped fins is investigated with parallel flow of cold water with hot air, the 4 internal fins configuration Nusselt Number is also determined with different mass flow rate.

**Table 13:** Showing the different values of Parallel Flow Temperature

Mass flow rate (Kg/s)	Sample 1
0.0197	7.28
0.0263	16.92
0.0329	25.61
0.0395	28.93

**Table 14:** Showing the different values of Parallel Flow Temperature

Mass flow rate (Kg/s)	Sample 2
0.0197	9.29
0.0263	18.87
0.0329	27.15
0.0395	31.12

**Table 15:** Showing the different values of Parallel Flow Temperature

Mass flow rate (Kg/s)	Sample 3
0.0197	8.12
0.0263	17.85
0.0329	26.93
0.0395	29.27

Here in this case the Nusselt Number at the outlet of the blossom shaped fins is investigated with counter flow of cold water with hot air, the 4 internal fins Nusselt Number is also determined with different mass flow.

**Table 16** Showing the different values of Counter Flow Nusselt Number

Mass flow rate (Kg/s)	Sample 1
0.0197	8.29
0.0263	17.24
0.0329	26.11
0.0395	29.96

**Table 17:** Showing the different values of Counter Flow Nusselt Number

Mass flow rate (Kg/s)	Sample 2
0.0197	10.83
0.0263	19.92
0.0329	29.23
0.0395	33.1

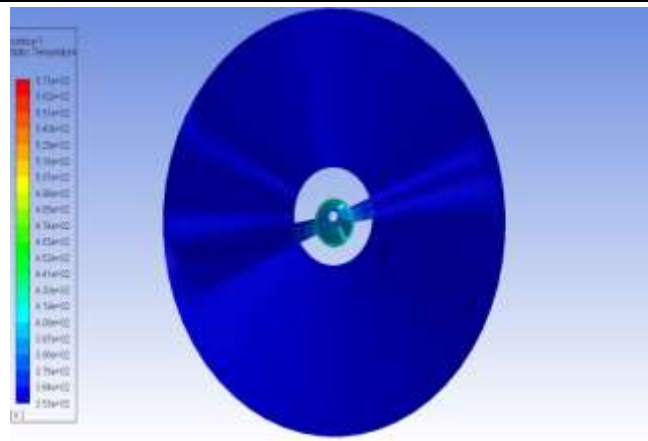


Figure 21: Counter Flow Air Static Temperature

Table 18: Showing the different values of Counter Flow Nusselt Number

Mass flow rate (Kg/s)	Sample 3
0.0197	9.35
0.0263	18.82
0.0329	27.33
0.0395	30.57

Table 19: Showing the different values of Parallel Flow Nusselt Number

Parallel Flow Nusselt Number			
Mass flow rate (Kg/s)	Sample 1	Sample 2	Sample 3
0.0197	7.28	9.29	8.12
0.0263	16.92	18.87	17.85
0.0329	25.61	27.15	26.93
0.0395	28.93	31.12	29.27

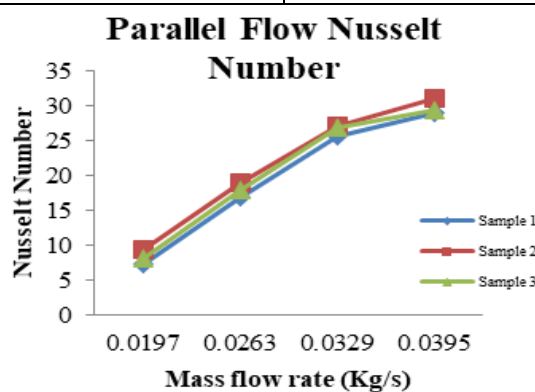
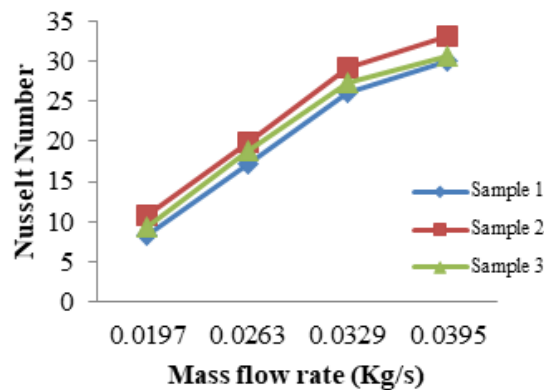


Figure 22: Parallel Flow Nusselt Number

Table 20 Showing the different values of Counter Flow Nusselt Number

Counter Flow Nusselt Number			
Mass flow rate (Kg/s)	Sample 1	Sample 2	Sample 3
0.0197	8.29	10.83	9.35
0.0263	17.24	19.92	18.82
0.0329	26.11	29.23	27.33
0.0395	29.96	33.1	30.57

**Counter Flow Nusselt Number**



**Figure 23: Counter Flow Nusselt Number**

Here in this case the Friction Factor at the outlet of the blossom shaped fins is investigated with parallel flow of cold water with hot air, the 4 internal fins Friction Factor is also determined with different mass flow rate.

**Table 21: Showing the different values of Parallel Flow Friction Factor**

Mass flow rate (Kg/s)	Sample 1
0.0197	0.024
0.0263	0.019
0.0329	0.016
0.0395	0.014

**Table 22: Showing the different values of Parallel Flow Friction Factor**

Mass flow rate (Kg/s)	Sample 2
0.0197	0.02
0.0263	0.016
0.0329	0.013
0.0395	0.011

**Table 23 Showing the different values of Parallel Flow Friction Factor**

Mass flow rate (Kg/s)	Sample 3
0.0197	0.022
0.0263	0.018
0.0329	0.015
0.0395	0.012

Here in this case the Friction Factor at the outlet of the blossom shaped fins is investigated with counter flow of cold water with hot air, the 4 internal fins Friction Factor is also determined with different mass flow.

**Table 24 Showing the different values of Counter Flow Friction Factor**

Mass flow rate (Kg/s)	Sample 1
0.0197	0.022
0.0263	0.017
0.0329	0.015
0.0395	0.012

**Table 25:** Showing the different values of Counter Flow Friction Factor

Mass flow rate (Kg/s)	Sample 2
0.0197	0.019
0.0263	0.015
0.0329	0.012
0.0395	0.011

**Table 26:** Showing the different values of Counter Flow Friction Factor

Mass flow rate (Kg/s)	Sample 3
0.0197	0.021
0.0263	0.017
0.0329	0.014
0.0395	0.012

**Table 27:** Showing the different values of Parallel Flow Friction Factor

Parallel Flow Friction Factor			
Mass flow rate (Kg/s)	Sample 1	Sample 2	Sample 3
0.0197	0.024	0.02	0.022
0.0263	0.019	0.016	0.018
0.0329	0.016	0.013	0.015
0.0395	0.014	0.011	0.012

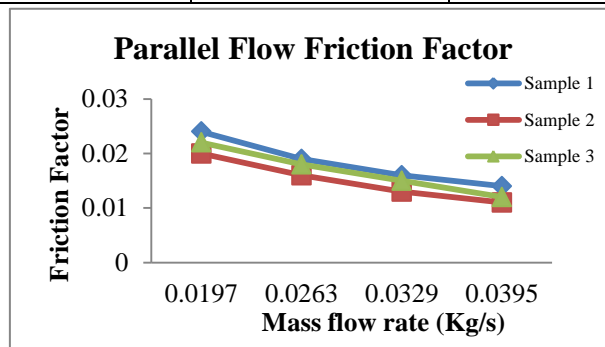


**Figure 24:** Parallel Flow Friction Factor

**Table 28:** Showing the different values of Counter Flow Friction Factor

Counter Flow Friction Factor			
Mass flow rate (Kg/s)	Sample 1	Sample 2	Sample 3
0.0197	0.022	0.019	0.021
0.0263	0.017	0.015	0.017
0.0329	0.015	0.012	0.014

0.0395	0.012	0.011	0.012
--------	-------	-------	-------

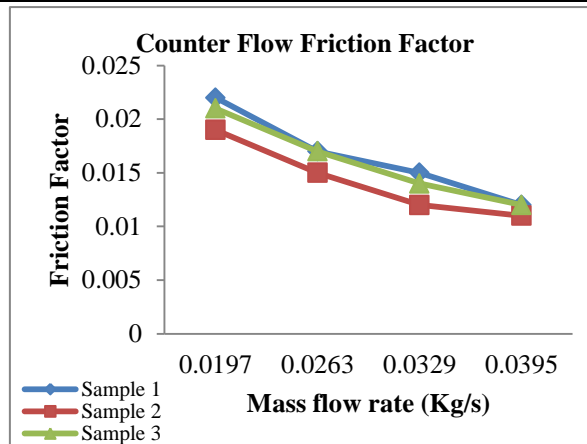


Figure 25: Counter Flow Friction Factor

## VI. CONCLUSION

In this work, numerical analysis is performed to investigate the parametric effects of the inner petaloid fins. A quantitative analysis was presented. The results show that various parameters influence the temperature distribution. Here we show the effect of the internal fin configuration. The Nusselt number and friction coefficient also show the effect of their variation on the fin configuration. In order to increase the heat transfer efficiency of the air in the system, it is necessary to find the optimum temperature distribution of the air, find the optimum fin configuration, and achieve the impetus for the water molecules. Increases heat transfer within the system. The above results conclude that Sample – 2 provides a higher temperature distribution in both co-current and counter-current at a mass flow rate of 0.0395 kg/s.

## VII. REFERENCES

- [1] Mohammad. Sikindar Baba, A.V.Sita Rama Raju, M. BhagvanthRao, Heat transfer enhancement and pressure drop of Fe<sub>3</sub>O<sub>4</sub> -water nanofluid in a double tube heat exchanger with internal longitudinal fins.
- [2] Evangelos Bellos, Christos Tzivanidis, Dimitrios Tsimpoukis, "Optimum number of internal fins in parabolic trough collectors, Applied Thermal Engineering 137 (2022) 669–677
- [3] Luanfang Duan, Xiang Ling, HaoPeng, Flow and heat transfer characteristics of a double-tube structure internal finned tube with blossom shape internal fins, Applied Thermal Engineering 128 (2018) 1102–1115.
- [4] M.J. Li, H. Zhang, J. Zhang, Y.T. Mu, E. Tian, D. Dan, X.D. Zhang, W.Q. Tao, "Experimental and numerical Study and Comparison of Performance for WavyFin and a Plain Fin with Radiantly Arranged Winglets around Each Tube in Finand-tube Heat Exchangers",
- [5] Swastik Acharya, Sukanta K. Dash, Natural convection heat transfer from a horizontal hollow cylinder with internal longitudinal fins, International Journal of Thermal Sciences 134 (2021) 40–539.
- [6] Guodong Qiu, Jian Sun, Yuanyang Ma, Jiagang Qu, WeihuaCai, Theoretical study on the heat transfer characteristics of a plain fin in the finned-tube evaporator assisted by solar energy, International Journal of Heat and Mass Transfer 127 (2018) 847–855.
- [7] Evangelos Bellos, Christos Tzivanidis, Dimitrios Tsimpoukis, "Optimum number of internal fins in parabolic trough collectors, Applied Thermal Engineering 137 (2019) 669–677
- [8] Mohammad Sepehr, Seyed Saeed Hashemi, Mohammad Rahjoo, Vahid Farhangmehr, Ashkan Alimoradi, "Prediction of heat transfer, pressure drop and entropy generation in shell and helically coiled finned tube heat exchangers".
- [9] Evangelos Bellos, Christos Tzivanidis, Dimitrios Tsimpoukis, Thermal enhancement of parabolic trough collector with internally finned absorbers, Solar Energy 157 (2017) 514–531.
- [10] Yong-Hui Wang, Ji-Li Zhang, Zhi-Xian Ma "Experimental study on single-phase flow in horizontal internal helically-finned tubes: the critical Reynolds number for turbulent flow,".



- 
- [11] Peilun Wang, Hua Yao, Zhipeng Lan, Zhijian Peng, Yun Huang, Yulong Ding, "Numerical investigation of PCM melting process in sleeve tube with internal fins" *Energy Conversion and Management* 110 (2016) 428–435.
- [12] Hao Peng, "Thermo-hydraulic performances of internally finned tube with a new type wave fin arrays.
- [13] Y. Naresh, C. Balaji, "Experimental investigations of heat transfer from an internally finned two phase closed thermosyphon".
- [14] Dong-Kwon Kim, "Thermal optimization of internally finned tube with variable fin thickness,"
- [15] Younghwan Joo, Sung Jin Kim, "Thermal optimization of vertically oriented, internally finned tubes in natural convection," *International Journal of Heat and Mass Transfer* 93 (2016) 991–999.
- [16] Alaa Ruhma Al-Badri, Andreas Bär, Achim Gotterbarm, Michael Heinrich Rausch, Andreas Paul Fröba, "The influence of fin structure and fin density on the condensation heat transfer of R134a on single finned tubes and in tube bundles," *International Journal of Heat and Mass Transfer* 100 (2016) 582–589.
- [17] José Fernández-Seara, Ángel Á. Pardiñas, Rubén Diz, "Heat transfer enhancement of ammonia pool boiling with an integral-fin tube,"
- [18] Min Zeng, Ting Ma, Bengt Sundén, Mohamed B. Trabia, Qiuwang Wang, "Effect of lateral fin profiles on stress performance of internally finned tubes in a high temperature heat exchanger," *Applied Thermal Engineering* 50 (2013) 886–895.
- [19] Yungang Wang, Qinxin Zhao, Qulan Zhou, Zijin Kang, Wenquan Tao, "Experimental and numerical studies on actual flue gas condensation heat transfer in a left-right symmetric internally finned tube," *International Journal of Heat and Mass Transfer* 64 (2013) 10–20.
- [20] A. Szajding, T. Telejko, R. Straka, A. Gołdasz, "Experimental and numerical determination of heat transfer coefficient between oil and outer surface of monometallic tubes finned on both sides with twisted internal longitudinal fins," *International Journal of Heat and Mass Transfer* 58 (2013) 395–401.